2018 IEEE/RSJ International Conference on Intelligent Robots and Systems (IROS)
Madrid, Spain, October 1-5, 2018

Soft Fabric Actuator for Robotic Applications

Sang Yul Yang[1] Kyeong Ho Cho[1], Youngeun Kim[1], Kihyeon Kim[1], Jae Hyeong Park[1], Ho Sang Jung[1], Jeong U Ko[1], Hyungpil Moon[1], Ja Choon Koo[1], Hugo Rodrigue[1], Ji Won Suk[1], Jae-do Nam[2], Hyouk Ryeol Choi[1], *Member, IEE*E

***Abstract*— This paper presents a fabric actuator consisting of ordinary polymer fibers, conductive fibers, and twisted and coiled soft actuators (TCAs). Previous studies have developed a Spandex TCA (STCA) that is driven at a lower temperature than the conventional Nylon TCA and exhibits greater actuation strain. However, no method to drive STCAs via electrical joule-heating has been developed yet. The fabric actuator presented in this paper offers a solution to this problem by employing an STCA multiple fabrication method, a continuous fabrication method, bundling technology, and weaving technology. Two types of samples (cylindrical and planar) are fabricated and their performances are evaluated experimentally. From the actuation test according to the loads, the maximum contraction strain of 34.3% is measured. The repeatability is also verified through 200 cycles of actuation. Using a linearized model, the dynamic performance of the fabric actuator is predicted and compared with experimental results. An actual human arm size mannequin is driven by applying the fabric actuator, and angle control can be achieved with an encoder mounted on the joint. In addition, fabric actuator is weaved to sweater showing the possibility of wearable assistive robot.**

I. INTRODUCTION

For many years, researchers have worked to develop devices capable of enhancing and rehabilitating human movement. Most of these devices employ motors, and have been sufficiently developed such that they can be used by people in practice [1], [2]. However, these motor-driven assistive devices are fundamentally problematic owing to their noisiness and heavy weight. A more practical and useful form of these assistive devices would be one that is lightweight and wearable. Various soft actuators such as dielectric elastomer actuators(DEA), shape memory alloys(SMA), and pneumatic artificial muscles have been developed to solve these aforementioned problems [3], [4], [5], [6], [7]. However, each actuator still requires addtional system, and has low stroke and high hysteresis to control. In case of DEA, it has low strain(under 10%, silicone), so additional pre-stretch systems for high stroke and strain should be needed. SMA has too high hysteresys to control. Hydraulic actuator has sufficient strain (up to 40%) but must require a pump .Thus, the use of these soft actuators is not enough to solve motor problems. Recently, lightweight twisted and coiled soft actuators (TCAs) have been developed using polymer fibers capable of generating high forces with low hysteresis [8]. These TCAs can be fabricated using inexpensive polymer materials and simple twisting processes. Furthermore, when a conductive coating is applied to the surface of the TCA, it becomes electrically drivable, which allows for the device to be controlled via small electronic systems [9], [10]. However, previous studies have shown that TCAs can only achieve low actuation strains at practical temperatures; higher temperatures are required to obtain useful actuation displacements. Using a mandrel to increase the diameter of the TCA coil has been shown to increase the achievable displacement; however, it also decreases the generated force, repeatability, and efficiency of the space [11].

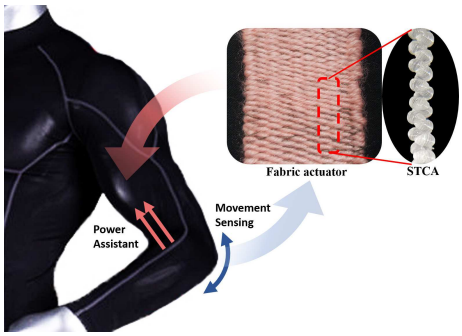

Fig. 1. Application of the fabric actuator. It can be used for artificial muscles and wearable robots

In our previous work, we developed a TCA using Spandex (SPX) that achieved large actuation strains at lower operating temperatures compared with TCAs made from the more commonly used nylon. SPX TCA (STCA), which can be fabricated without a mandrel, has up to 45% contraction strain at 130 C, and approximately 1500 J / kg specific work [12]. These performance metrics are high compared to the contraction rate of human muscle, which is 20%–30%, and the specific work of human muscle, which is approximately 39 J / kg [13]. When using nylon TCAs (NTCAs) for applications in which the actuation strain is low, a long TCA is needed to achieve the target displacement [14], [15]. Research has been conducted to develop a mechanism that would allow shorter NTCAs to accumulate displacements and avoid the need for long NTCAs [16]. However, such a mechanism is unnecessary when utilizing STCAs, because a short STCA can achieve the large displacements required in practical applications.

If an electrically driven fabric-type actuator is developed, it can have many practical applications. For example, it could be used to develop wearable robots in the form of clothes,

[1] the School of Mechanical Engineering [2] Department of Polymer Science and Engineering, Sungkyunkwan University, Chunchon-dong 300, Suwon, Republic of Korea. All the correspondences are delivered to Prof. H. R. Choi hrchoi@me.skku.ac.kr

and it also can be applied to various systems in a module form (Fig. 1). This fabric-type actuator can be developed through STCA by taking advantage of the fact that TCAs are fiber based. In addition, the fabric-type actuator can solve the problem that STCAs alone cannot be driven by electric joule-heating because conductive coatings for STCA have not yet been developed. When TCA and electro-conductive fibers are used together as the fabric, the TCA can be driven by electric joule-heating through the electro-conductive fibers [9], [10]. The heat generated from the conductive fibers transfers to and drives the TCAs.

Weaving and knitting are typical textile fabrication methods. Previous studies have used knitted SPX in the creation of actuators and sensors [17]. In these studies, the SPX was fabricated using a bare, uncoiled fiber that exhibits a small actuation strain (up to 13% actuation strain normalized with respect to the loaded muscle length). If knitting is performed with STCAs, a larger actuation displacement may be observed. Knitting generally requires a long thread and the advanced skill of handling a crochet hook or bamboo needle. Conversely, the weaving method can be performed by a long thread or several same length threads, and it does not require advanced skill. In addition, a fabric can be fabricated with diverse kinds of threads by weaving. The STCA fabrication device that simultaneously produces multiple TCAs was developed in our previous research [12]. In this study, an STCA continuous fabrication device is developed. Therefore, the fabric actuator was fabricated with multiple short length STCAs or a long length STCAs and additional functional threads by using the weaving method. This paper presents a high-performance fabric actuator that can be electrically driven. To create this fabric actuator, we employed STCA fabrication methods, bundling methods, and textile fabrication methods. In Section II, the overall fabric actuator fabrication process is explained step by step. In Section III, the fabric actuator performance evaluation equipment are introduced, and the actuation performance of the fabric actuator is evaluated. In Section IV, we demonstrate the application of fabric actuator as a wearable device. Finally, the conclusion is given in Section V.

II. Fabrication of Fabric Actuator

A. *STCA fabrication and bundling methods*

The fabric actuator is composed of STCA, electroconductive fiber, thermal conducting fiber, and connectors. Because the STCA is fabricated with SPX fiber, which has very soft properties (ultrastretchable and low stiffness [18]), two coil processes are required for STCA fabrication, unlike NTCA, which is fabricated with a one coil process [8], [11]. STCA fabrication and bundling can be proceeded with two approaches as follows.

1) Approach 1 : using multiple short length STCAs: The previous STCA fabrication device fabricates multiple short length STCAs with multiple rotors at once [12]. As shown in Fig. 2(a), the SPX fiber (Creora, Hyosung Co.) is prepared to be the required length and both ends are tied together. The resulting loop is folded twice to create four loops (8 fibers).

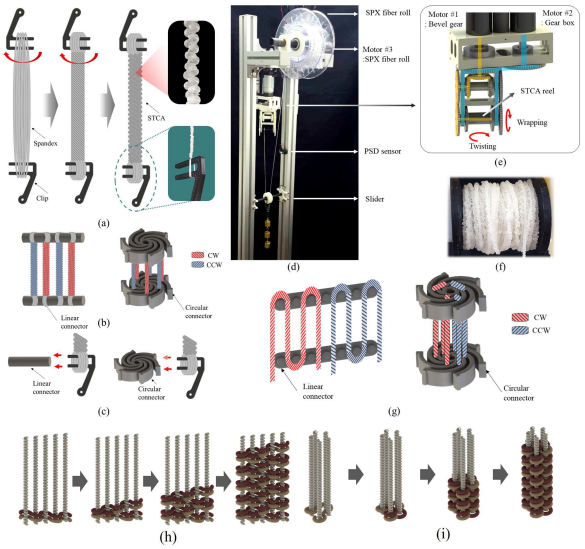

Fig. 2. (a)Fabrication of multiple short length STCA (b) preventing releasing torque (c) method to move ring into connector (d) STCA continuous fabrication device (e)device main fabrication mechanism (f) fabricated long STCA (g) bundling method for a long STCA (h) Planar weaving process, (b) Cylindrical weaving process.

Then, the four loops are connected to F-shaped clips, and the fibers are twisted until two coil processes are completed. The STCA bundle can be made into any shape (e.g., linear or circular) by hanging the fabricated multiple STCAs on various connectors (Fig. 2(b)). In the hanging process, the multiple STCAs can be easily hung on a connector by using F-shaped clips (Fig. 2(c)). As STCA is fabricated by twist-insertion, it basically generates the releasing torque by the restoring force of the SPX fiber after twist-insertion. When making the STCA bundle, if all the twisted directions of the STCA are the same, the parallel arrangement of the STCAs is broken and the driving force is mitigated owing to the releasing torque. Bare SPX is not self-twisted and can be manufactured in all directions (i.e., clockwise (CW), counter clockwise (CCW)). In the bundling process, the releasing torques can be cancelled out by using two types of STCAs fabricated in different directions, and it is able to maintain the bundled forms of STCA. Therefore, the STCAs fabricated with CW and CCW directions are used in equal amounts in an STCA bundle as shown in Fig. 2(b).

In approach 1, An STCA continuous fabrication device was newly developed, as shown in Fig. 2(d). The position sensitive detector (PSD) sensor measures the distance between the slider and itself, and motor #3 releases or winds the SPX fiber roll depending on the distance. The SPX fiber of the roll is connected to the STCA reel through the slider. By loading a suitable weight to the slider, the SPX fiber has a constant tension for twist-insertion. The main fabrication mechanism consists of motor #1 and #2, the differential gear, and the STCA reel as shown in Fig. 2(e). Motor 1 rotates the bevel gear inside of the differential gear, and motor #2 rotates the differential gear box through the spur gear. By

the difference in RPMs of motor #1 and #2, the STCA reel can perform twisting and wrapping. When motor #1 and #2 rotate in an inverse direction with the same RPM, the STCA reel performs twisting only. When motors #1 and #2 rotate in an inverse direction with different RPMs, the STCA reel performs both twisting and wrapping. Through this fabrication device, continuous STCA fabrication is possible, and a long length STCA was fabricated as shown in Fig. 2(f). For generating an anti-releasing torque, two long length STCAs in CW and CCW directions are prepared. By connecting these long length STCAs to the upper and lower connectors in a zigzag pattern, the bundling process is simplified and quickly completed as shown in Fig. 2(g). The fabric made in a planar form uses a bundle arranged in a line and the method shown in Fig. 2(h). Weaving is carried out using electro-conductive fibers (# 260151023534, Shieldex, Statex Co.) and ordinary fibers (acrylic fiber in this paper) as warp, and STCAs as weft. The warp yarns are alternately zigzagged in the weft yarns. Electro-conductive fibers are electrically joule-heated and are used to drive the STCAs. In addition, ordinary fibers spread the heat generated from the electro-conductive fibers evenly, forming a cloth-like shape. The fabric actuator made in a cylindrical shape uses a bundle arranged in a circle; the method illustrated in Fig. 2 (i) is used. The actuator is made of the same material as the planar-type fabric. The process of interlacing warp yarns alternately with zigzags is similar. However, for the planar shape, the process proceeds alternately to the left and the right, while for the cylindrical shape, the process proceeds in a spiral direction.

III. Actuation Test

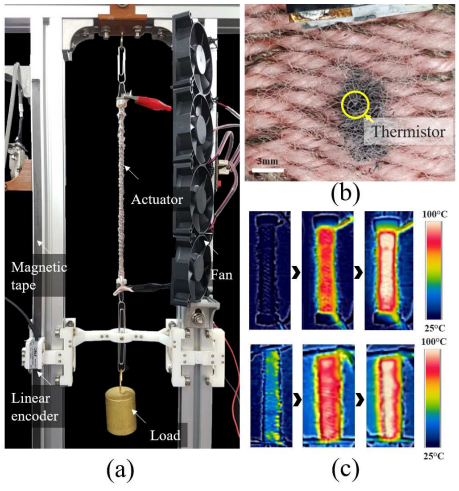

Fig. 3. (a) Performance evaluation equipment; (b) embedded thermistor; (c) surface temperature images taken by a thermal camera

A. Experimental equipment and samples

Figure 3 shows the equipment used in the performance evaluation experiment. The displacement was measured using a magnetic tape and a slider with a linear encoder (LM10, RLS). The resolution of the encoder was 0.01 mm. The weight of the slider was 250 g, including the encoder. Friction was minimized using a bearing. The temperature of the actuator was measured with a thermistor (111-103EAJ-H01, Honeywell) and a thermal camera (E5, FLIR System). The thermistor was attached to the actuator with thermal grease (Cooling Flow - CT250, Coolertec) [19]. All systems were controlled via LabVIEW, a DAQ (NI USB-6341, National Instruments), and solid-state relays. The data was also received via LabVIEW. Two types of samples were used in the experiment: planar and cylindrical samples. STCAs for samples were fabricated with a 2.75 N load and 5200 rotations/m. Three experiments were conducted to measure the performance depending on the load, the repeatability, and the performance according to the temperature. Furthermore, the performance according to the temperature was predicted by the linear model and compared with the experimental results.

B. Actuation performance results

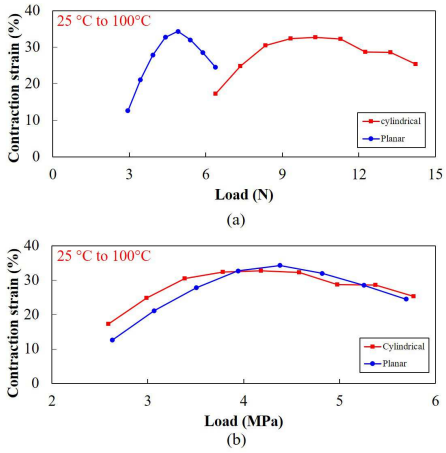

Fig. 4. (a) Contraction strain by actuation force of load(N) (b) Contraction strain by actuation stress(MPa)

Performance evaluation tests were conducted with various loads to find the maximum contraction strain and optimal load condition (Fig. 4(a)). The fabric actuator was driven by joule-heating between 25°C and 100°C. The maximum contraction strain of the cylindrical sample was 32.7% with a 10.3 N load, and the maximum contraction strain of the planar sample was 34.3% with a 4.91 N load. Load (MPa) is calculated by dividing Load (N) by the sum of the cross-sectional area of the STCA. The diameter of one strand of STCA is 534 μm [13], and the cross-sectional area is 0.224 mm^2. Depending on the performance of the STCA strand, the performance of the fabric actuator according to Load (MPa) is similar to that shown in Fig. 4(b). If more than 30% strain is considered as the optimal load section, the column type with many STCA has a wider load section. Increasing the number of strands in the STCA bundle will increase the optimum load (N) section. It is simple to fabricate an actuator which has the optimum load condition

TABLE I

SAMPLE PROPERTIES

Type	Length of wrap (mm)		Weft(STCA)		Total	
	Shieldex	Acrylic Fiber	Length of SPX(mm)	Number of STCAs	Resistance (Ohm)	Initial Length(mm)
Planar	1640	1820	500	5	47∼60	36
Cylindrical	1430	1790	500	11	73∼77	40

required. The load condition depends on Weft(STCA). The optimal load range of a single STCA is about 0.7 N to 1.1 N. As described above, STCA can be mounted on the connector as much as necessary for the connector. If 10N load conditions are required, weaving with 9 to 14 stranded STCA bundles.

Figure 5 shows the results of the repeatability test. Tests were conducted for 200 cycles with joule-heating and fan cooling. The cylindrical sample was heated by 6 W power for 8 s and cooled by fans for 35 s (Fig. 5(a)). The The planar sample was also heated by 6 W Power for 12 s and cooled by fans for 30 s(Fig. 5(b)). It was repeatedly driven between about 60°C and 26°C. The loads were 7.35 N for the cylindrical type and 3.92 N for the flat type, respectively. The ambient temperature was 26.2°C. Data were collected at 0.5 second intervals. Both results show that the maximum contraction strain varied within 1% for 200 cycles (8600 s in the cylindrical sample and 8400 s in the planar sample). But if the actuator is repeatedly driven with a full stroke, it is not fully recovered and slowly sag (Fig. 5(c)). The full stroke test was tested with cylindrical sample between 26°C and 100°C. The maximum contraction strain was changed 1% per 50 cycles (time : 5100s).

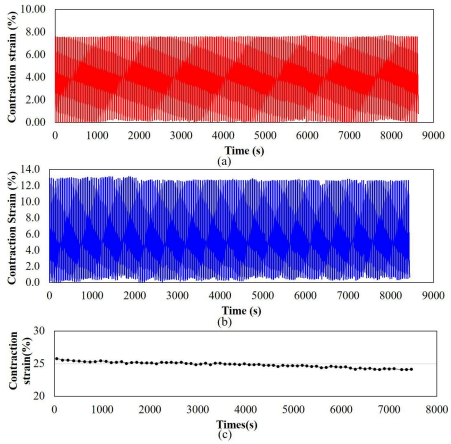

Fig. 5. (a) shows the repeatability test of the cylindrical fabric sample, and (b) shows the repeatability test of the planar fabric sample. Both illustrate the performance over 200 cycles. (c) Contracted strain at 100°C in repetitive actuation

C. Linear model and dynamic performance

A simple linear model is applied to show the characteristics and controllability of the actuator. The model which consists of a load, spring, and damper used to predict the

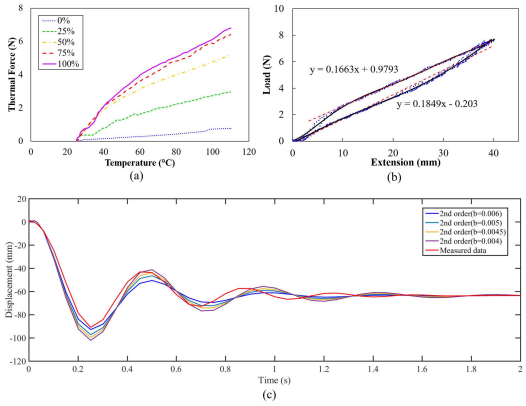

Fig. 6. (a) Thermal forces generated by heat were measured. The thermal force depends on the stretch length of the fabric actuator, and the graph shows the results for the five steps(0%,5%,25%,50%,75%,100%; (b) loads were measured during stretching and releasing the samples; (c) dynamic responses were measured by dropping a load of 9.31 N.

dynamic performance of the fabric actuator [15], [19]. Several assumptions were made for the model; it was assumed that the spring coefficient of the STCA was linear and that the dynamic response followed a spring-damper second order system. The final goal of the model was to predict the temperature-dependent displacement, and the formula is

$$m\Delta\ddot{x} = F_T + F_k - F_L - F_D \tag{1}$$

where F_T is a thermally generated force, F_k is spring force, F_L is load, and F_D is damping force. First, in order to obtain the thermal force, the temperature-dependent force was measured while changing the stretch length of the fabric actuator (Fig. 6(a)). The load applied at room temperature is assumed to be caused by the spring force, and the force generated by heat is set to zero. As the stretch of the fabric actuator increased, the heat increased the force further. Moreover, the increasing force tended to converge as the tensile ratio increased. The spring coefficient of k was obtained from the load-extension test (Fig. 6(b)). There is some hysteresis between stretching and releasing. In this paper, the tension graph during releasing was used to predict the contraction performance of the fabric actuator. The spring coefficient (k) was found to be 0.1849 N/m. The load drop experiment was carried out to obtain the damping force (Fig. 6(c)). The dynamic response was measured by applying a load of 9.31 N to the cylindrical type and dropping it. By fitting the response (2) with a mass-spring-damper second-order model, the damping coefficient (b) was obtained [15]. In the model fitted closest to the experimental result, the

damping coefficient was found to be 0.0045 $N \cdot s/mm$.

$$m\Delta\ddot{x} = k\left(x - x_0\right) - b\dot{x} \tag{2}$$

The performance of the cylindrical sample according to temperature was measured with the 9.31 N load. The experimental results and the performance predicted by the designed linear model are compared in Figure 7.

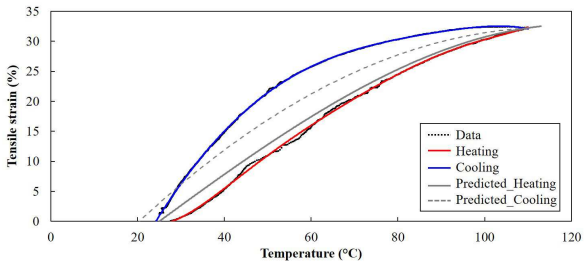

Fig. 7. Contraction strain was measured according to temperature. The predicted strain is plotted by the designed linear model

The predicted performance by the model during contraction is shown in gray line of Fig. 7, and a strain error of up to about 3% with the heating graph was found. But it showed a large deviation from the performance in cooling. Using the model during extension shown in gray dotted line, error for cooling performance gets smaller. But the error in cooling case is lager than heating. Heat is generated from the inside and spreads evenly, but there is a temperature difference between inside and outside at the time of cooling. This gap of temperature makes lager error. Also the model considered spring force as linear. The modulus of elasticity of the polymer fiber is changed every moment and the error is caused by this. If a model for the fabric actuator is developed including characteristics of wrap, such as a nonlinear model tracking actuation of the TCA, the hysteresis error of the fabric will be significantly reduced [20].

IV. Application and Discussion

A. Mannequin and assistant actuation

To verify the practicality of the fabric actuator, it was applied to a human arm mannequin (Fig. 8(a)). The mannequin was designed based on the size of an actual human arm. The joint of the mannequin is equipped with rotary encoders to measure the angle of the arms. The skeleton of the mannequin is made of carbon fiber, and the body is made of 3D-printed components. The used fabric actuator consists of 12 strands of STCA, with an initial length of 12 cm and a diameter of 6 mm. Mannequin-assistant actuation with the fabric actuator was conducted with encoder-feedback control (supplementary video). The 145.5 g box was attached to the mannequin hand for the test. The initial angle was 29°, and the experiment was carried out with the desired input at 40°, 50° and 60°. Figure 8(b) shows the test result. Also, Figure 8(c) shows the error between desired angle and actual angle. Mean Absolute error was calculated for each desired angular section. In other application shown in Fig. 9, planar type fabric actuator is weaved with sweaters and installed to

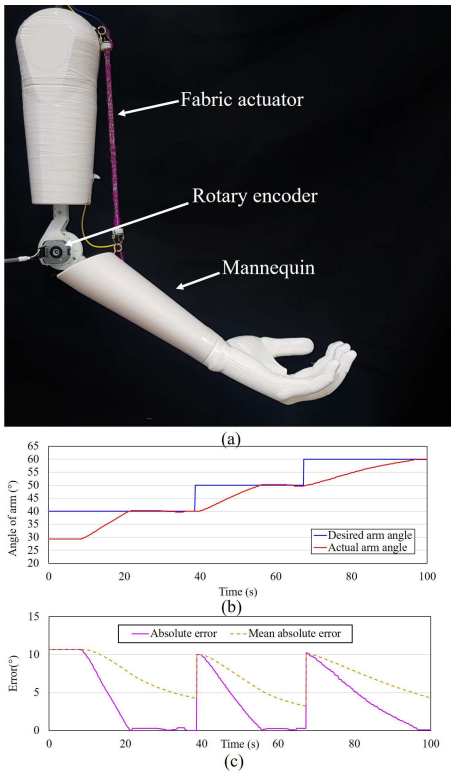

Fig. 8. (a) Mannequin configuration with a rotary encoder, a fabric actuator, 3D printed parts (b) joint angle data in actuation with feedback control (c) Absolute error between desired angle and actual angle & Mean absolute error between desired angle and actual angle

the human arm size mannequin which can rotate freely. The used planar type fabric actuator also consists of 12 strands of STCA. The sweater is generally used one and made of acrylic fiber. To transmit force generated by the actuator, the fabric actuator attached to mannequin. From the result, the sweatered mannequin can be bent from 20 to 90 through the fabric actuator without load.

B. Discussion

The problem of electrical driving, which is a disadvantage of high performance STCA, can be solved by utilizing STCA as a fabric. And by adopting STCA, large actuation displacement can be seen at a small temperature. Still, there is a problem that the actuation temperature is too high to contact human skin directly. A superficial solution is to put the insulation between the skin and the actuator, and a fundamental solution would be to lower the drive temperature. As with lowering the actuation temperature by changing the material of the TCA from Nylon to Spandex, research for temperature continues.

Common fibers in the warp yarns deliver heat evenly, but slow down the cooling rate. This paper tried to show the versatility by fabricating with general fiber. Therefore, the actuator can be fabricated through various materials, and the cooling rate changes depending on the thermal characteristics of the material used. Future research will be carried out to

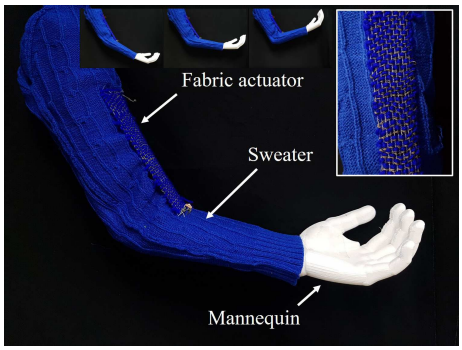

Fig. 9. (a) Sweatered Mannequin configuration with Fabric actuator, Sweater. Inserted image shows weaved fabric actuator to sweater. Without load, Mannequin can be driven by fabric actuator from 20° to 90°.

reduce the cooling rate of the fabric actuator by applying a fiber material that can quickly draw the heat of the actuator like a heat sink.

The optimal mechanical configuration of the actuator shown in this paper requires insulation from the skin and a lightweight cooling fan (if fast actuation needed). Through this actuator, a lightweight and simple structure robot compared to the previous wearable robot can be produced.

V. CONCLUSIONS

The fabric actuator was developed based on STCA with a conductive thread and ordinary thread. The fabric actuator could solve the electric driving problem of STCAs, and higher performance was exhibited. In this paper, it has been shown that fabric actuators can be fabricated in various forms, and two kinds of samples, cylindrical and planar type, were fabricated and tested. The maximum contraction strain of 34.3% was measured at 100 C , and the repeatability was confirmed by actuation over 200 cycles. The actuator was proven to be controllable by the linear model. The human arm mannequin was able to be driven by the fabric actuator and angle control was possible with a rotary encoder.

ACKNOWLEDGMENTS

This research was supported by the Convergence Technology Development Program for Bionic Arm through the National Research Foundation of Korea(NRF) funded by the Ministry of Science, ICT & Future Planning (no. 2014M3C1B2048175).

REFERENCES

[1] L. Cappello, A. Pirrera, P. Weaver, and L. Masia, "A series elastic composite actuator for soft arm exosuits," in *2015 IEEE International Conference on Rehabilitation Robotics (ICORR)*, Aug 2015, pp. 61–66.

[2] A. T. Asbeck, R. J. Dyer, A. F. Larusson, and C. J. Walsh, "Biologically-inspired soft exosuit," in *2013 IEEE 13th International Conference on Rehabilitation Robotics (ICORR)*, June 2013, pp. 1–8.

[3] F. Daerden and D. Lefeber, "Pneumatic artificial muscles: actuators for robotics and automation," *European journal of mechanical and environmental engineering*, vol. 47, no. 1, pp. 11–21, 2002.

[4] H. S. Jung, S. Y. Yang, K. H. Cho, M. G. Song, C. T. Nguyen, H. Phung, U. Kim, H. Moon, J. C. Koo, J.-D. Nam, and H. R. Choi, "Design and fabrication of twisted monolithic dielectric elastomer actuator," *International Journal of Control, Automation and Systems*, vol. 15, no. 1, pp. 25–35, 2017.

[5] H. R. Choi, K. Jung, N. H. Chuc, M. Jung, I. Koo, J. Koo, J. Lee, J. Lee, J. Nam, M. Cho, and Y. Lee, "Effects of prestrain on behavior of dielectric elastomer actuator," in *Proc. SPIE*, vol. 5759, no. 10.1117, 2005, pp. 12–599 363.

[6] P. Brochu and Q. Pei, "Advances in dielectric elastomers for actuators and artificial muscles," *Macromolecular rapid communications*, vol. 31, no. 1, pp. 10–36, 2010.

[7] H. Rodrigue, W. Wang, M.-W. Han, T. J. Kim, and S.-H. Ahn, "An overview of shape memory alloy-coupled actuators and robots," *Soft Robotics*, vol. 4, no. 1, pp. 3–15, 2017.

[8] C. S. Haines, M. D. Lima, N. Li, G. M. Spinks, J. Foroughi, J. D. W. Madden, S. H. Kim, S. Fang, M. Jung de Andrade, F. Göktepe, Ö. Göktepe, S. M. Mirvakili, S. Naficy, X. Lepró, J. Oh, M. E. Kozlov, S. J. Kim, X. Xu, B. J. Swedlove, G. G. Wallace, and R. H. Baughman, "Artificial muscles from fishing line and sewing thread," *Science*, vol. 343, no. 6173, pp. 868–872, 2014. [Online]. Available: http://science.sciencemag.org/content/343/6173/868

[9] S. M. Mirvakili, A. Rafie Ravandi, I. W. Hunter, C. S. Haines, N. Li, J. Foroughi, S. Naficy, G. M. Spinks, R. H. Baughman, and J. D. Madden, "Simple and strong: Twisted silver painted nylon artificial muscle actuated by joule heating." SPIE, 2014.

[10] J. Park, J. W. Yoo, H. W. Seo, Y. Lee, J. Suhr, H. Moon, J. C. Koo, H. R. Choi, R. Hunt, K. J. Kim, S. H. Kim, and J.-D. Nam, "Electrically controllable twisted-coiled artificial muscle actuators using surface-modified polyester fibers," *Smart Materials and Structures*, vol. 26, no. 3, p. 035048, 2017.

[11] C. S. Haines, N. Li, G. M. Spinks, A. E. Aliev, J. Di, and R. H. Baughman, "New twist on artificial muscles," *Proceedings of the National Academy of Sciences*, p. 201605273, 2016.

[12] S. Y. Yang, K. H. Cho, Y. Kim, M.-G. Song, H. S. Jung, J. W. Yoo, H. Moon, J. C. Koo, J. do Nam, and H. R. Choi, "High performance twisted and coiled soft actuator with spandex fiber for artificial muscles," *Smart Materials and Structures*, vol. 26, no. 10, p. 105025, 2017. [Online]. Available: http://stacks.iop.org/0964-1726/26/i=10/a=105025

[13] I. W. Hunter and S. Lafontaine, "A comparison of muscle with artificial actuators," in *Solid-State Sensor and Actuator Workshop, 1992. 5th Technical Digest., IEEE*. IEEE, 1992, pp. 178–185.

[14] K. H. Cho, M. G. Song, H. Jung, J. Park, H. Moon, J. C. Koo, J. Nam, and H. R. Choi, "A robotic finger driven by twisted and coiled polymer actuator," *SPIE Smart Structures and Materials+ Nondestructive Evaluation and Health Monitoring*, pp. 97 981J–97 981J, 2016.

[15] M. C. Yip and G. Niemeyer, "High-performance robotic muscles from conductive nylon sewing thread," in *Robotics and Automation (ICRA), 2015 IEEE International Conference on*. IEEE, 2015, pp. 2313–2318.

[16] K. H. Cho, M. G. Song, H. Jung, S. Y. Yang, H. Rodrigue, H. Moon, J. C. Koo, and H. R. Choi, "Biomimetic robotic joint mechanism driven by soft linear actuators," in *Robotics and Automation (ICRA), 2017 IEEE International Conference on*. IEEE, 2017, pp. 1850–1855.

[17] J. Foroughi, G. M. Spinks, S. Aziz, A. Mirabedini, A. Jeiranikhameneh, G. G. Wallace, M. E. Kozlov, and R. H. Baughman, "Knitted carbon-nanotube-sheath/spandex-core elastomeric yarns for artificial muscles and strain sensing," *ACS nano*, vol. 10, no. 10, pp. 9129–9135, 2016.

[18] E. M. Hicks, A. J. Ultee, and J. Drougas, "Spandex elastic fibers," *Science*, vol. 147, no. 3656, pp. 373–379, 1965.

[19] K. H. Cho, M.-G. Song, H. Jung, S. Y. Yang, H. Moon, J. C. Koo, and H. R. Choi, "Fabrication and modeling of temperature-controllable artificial muscle actuator," in *Biomedical Robotics and Biomechatronics (BioRob), 2016 6th IEEE International Conference on*. IEEE, 2016, pp. 94–98.

[20] T. A. Luong, S. Seo, J. C. Koo, H. R. Choi, and H. Moon, "Differential hysteresis modeling with adaptive parameter estimation of a super-coiled polymer actuator," in *Ubiquitous Robots and Ambient Intelligence (URAI), 2017 14th International Conference on*. IEEE, 2017, pp. 607–612.